



Three approaches to evaluate the heat dissipated during fatigue crack propagation experiments

A. Vedernikova, A. Iziumova, A. Vshivkov, O. Plekhov

Institute of Continuous Media Mechanics UB RAS, 614013 Perm, Russia

terekhina.d@icmm.ru, <https://orcid.org/0000-0003-1069-7887>

fedorova@icmm.ru, <https://orcid.org/0000-0002-1769-9175>

vshivkov.a@icmm.ru, <https://orcid.org/0000-0002-7667-455X>

poa@icmm.ru, <https://orcid.org/0000-0002-0378-8249>

ABSTRACT. This work is devoted to the comparative analysis of three techniques for measurement of energy dissipation in metals under fatigue crack propagation: use of original contact heat flux sensor, post-processing of infrared thermography data and lock-in thermography. Contact heat flux sensors allow real-time recording of heat source values. Non-contact temperature measurements by infrared thermography techniques make it possible to calculate the heat source field on the specimen surface by solving a heat conductivity equation. Lock-in thermography is a well-established technique for measuring energy dissipation under cyclic loading conditions based on the analysis of the second harmonic amplitude of the thermal signal. This paper describes the results of the experiments with V-notched flat specimens made of stainless steel AISI 304 which were subjected to cyclic loading. It was shown that the values of energy dissipation estimated by different techniques are in good qualitative agreement. Contact and non-contact measurements can be used for investigation of energy dissipation either separately or in combination. Based on the measurements, the power dependence of fatigue crack growth rate on dissipated heat near the crack tip can be obtained.

KEYWORDS. IR-thermography; Lock-in thermography; Heat flux sensor; Dissipated energy; Fatigue crack propagation.



Citation: Vedernikova, A., Iziumova, A., Vshivkov, A., Plekhov, O., Three approaches to evaluate the heat dissipated during fatigue crack propagation experiments, *Frattura ed Integrità Strutturale*, 51 (2020) 1-8.

Received: 27.08.2019

Accepted: 08.10.2019

Published: 01.01.2020

Copyright: © 2020 This is an open access article under the terms of the CC-BY 4.0, which permits unrestricted use, distribution, and reproduction in any medium, provided the original author and source are credited.

INTRODUCTION

One of the key problems of fracture mechanics and strength analysis is to predict the fatigue life of cracked parts of engineering constructions subjected to cyclic loading. The fatigue crack growth well correlates with energy dissipation at the crack tip [1-25]. Different experimental approaches focused on the experimental study of the dissipated energy are described in the literature.



One of the techniques is based on the application of original Seebeck effect-based contact heat flux sensor, which ensures the quantitative integral heat flow values in some area near the crack tip. Such methodology was originally used for studying energy dissipation in liquid flows [3] and the failure of metals [2, 4].

The second method for heat flux estimation involves analysis of temperature distribution measurements obtained for the specimen surface by means of infrared (IR) thermography. Plastic strain-induced heat sources were calculated by solving the volume-averaged heat conduction equation. The main difficulties associated with application of the second technique can be attributed to the necessity to differentiate strongly oscillating signals and to determine the parameters responsible for the interaction between the specimen and the external environment. Nevertheless, IR thermography data are widely used to gain deeper insight in the process of plastic deformation and fracture of metallic materials [5-10].

It was shown in [11, 12] that the results of contact (heat flux sensor) and non-contact (IR thermography) measurements of energy dissipation during irreversible deformation agree well.

The third, lock-in thermography, method provides space-resolved measurements, extracts thermoelastic information directly from the thermal signal [13] and investigates energy dissipation using the double frequency method proposed by Sakagami [14]. Lock-in thermography is employed to detect crack initiation and propagation in structural materials using thermographic mapping [15-25].

In this study, we have shown that the energy dissipation values measured by the thermography techniques are in good qualitative agreement with the results obtained by the method in which contact heat flux sensors are used. This provides evidence that contact and non-contact measurements can be used either separately (fast assessment of the material state at different loading stages) or in combination (verification of the heat source value and estimation of its distribution over the material surface).

EXPERIMENTAL

A series of tests were performed on V-notched flat specimens made of stainless steel AISI 304 and subjected to cyclic loading at a frequency of 10 Hz (constant stress amplitude 12 kN and stress ratio $R = 0$). Fig. 1 shows the geometry of the specimens and the experimental setup scheme. The chemical composition of the material examined is given in Tab. 1.

C	Cr	Fe	Mn	Ni	P	S	Si
0.08	18-20	66.34-74	2	8-10.5	0.045	0.03	1

Table 1: Chemical composition (wt. %) of stainless steel AISI 304.

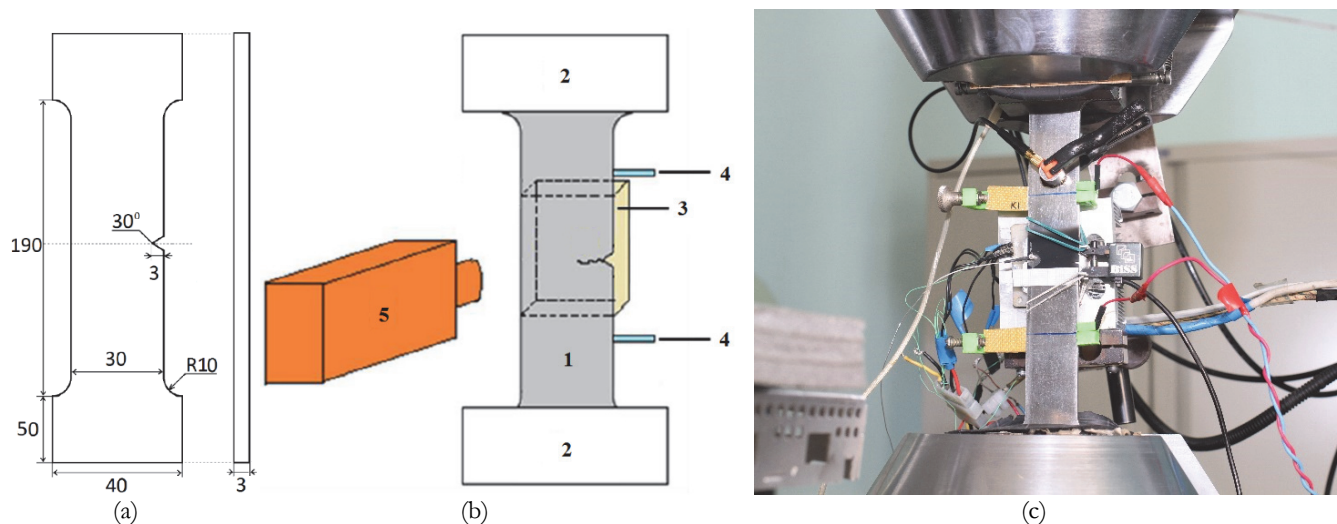


Figure 1: (a) specimen geometry; (b) schematic of the measuring equipment: 1 – test specimen, 2 – grips of the testing machine, 3 – contact heat flux sensor, 4 – potential drop measuring setup to monitor the crack length, 5 – infrared camera; (c) photo of the specimen and the measuring equipment.



Specimens were cyclic loaded in a servohydraulic testing machine Instron 8802. The potential drop technique was used to measure and characterize the crack propagation process [26]. Crack sizes in a steel specimen were predicted by applying a constant direct current or an alternating current to the specimen and by measuring an increase in electrical resistance due to the crack propagation.

To analyze the energy dissipation at the crack tip during mechanical tests, we have used the Seebeck effect-based heat flux sensor. In order to improve the heat flow, a heat-conductive paste was applied to the specimen surface beneath the sensor. The evolution of the temperature field was recorded with an infrared camera FLIR SC 5000. The features of the IR camera are as follows: the spectral range of 3-5 μm , the maximum frame size is 320×256 pixels, the spatial resolution is 10⁻⁴ meters, and the temperature sensitivity is in the range from 25 mK to 300 K. The camera was calibrated based on the standard calibration table. The application of the LIRSC5000 MW G1 F/3.0 close-up lens (with distortion less than 0.5%) made it possible to investigate the plastic zone in detail.

The specimen surface intended for infrared shooting was polished in several stages and coated by a thin layer of amorphous carbon to improve the surface emissivity. Specimens were tested and monitored by means of the infrared camera in order to acquire thermographic sequences during tests at regular intervals (1000 cycles each).

DIRECT HEAT FLUX MEASUREMENT TECHNIQUE

The heat flux measurement technique relies on the use of Seebeck effect-based contact heat flux sensor [2]. The heat dissipated by specimens is directly proportional to the current intensity and the time it takes for the current to pass through the specimens:

$$P = \Pi_{AB} I \quad (1)$$

where P is the heat flux power (W), I is the direct current (A), and Π_{AB} is the Peltier coefficient (V), which is related with a coefficient of thermal electromotive force.

Structurally, the sensor comprises two Peltier elements ("measuring" and "cooling"), thermocouples, and a radiator. To measure the heat flow through the "measuring" Peltier element during the experiment, the temperature on its free surface is kept constant. The cooling Peltier element caulked with a radiator was connected with the "measuring" Peltier element. This cooling system has feedback and is controlled based on two temperature sensors located between "measuring" and cooling Peltier elements and far from the studied specimen in the zone with constant temperature. The heat flux emitted from the specimen surface passes through the heat flux sensor. The sensor was fixed on the specimens by applying thermal paste and then pressed against the spring to provide the necessary thermal contact. The negligibility of heat dissipation which was caused by sensor – specimen friction was experimentally proved [2]. The signal from the flux sensor was measured by the amplifier and registered in the ADC of the microcontroller. Then the data were transmitted to personal computer for further processing. The sensors were calibrated using a device with a controlled heat flux.

INDIRECT HEAT FLUX MEASUREMENT TECHNIQUE

Estimation of the heat sources field based on the heat conductivity equation

To calculate the heat source field induced by plastic deformation, we use heat conduction Eqn. (2) for processing the obtained infrared thermography data:

$$\rho c \frac{\partial T(x, y, z, t)}{\partial t} = Q(x, y, z, t) + k \left(\frac{\partial^2 T(x, y, z, t)}{\partial x^2} + \frac{\partial^2 T(x, y, z, t)}{\partial y^2} + \frac{\partial^2 T(x, y, z, t)}{\partial z^2} \right) \quad (2)$$

where $T(x, y, z, t)$ is the temperature field, ρ is the material density (kg/m^3), c is the heat capacity ($\text{J}/(\text{kg}\cdot\text{K})$), k is the heat conductivity ($\text{W}/(\text{m}\cdot\text{K})$), $Q(x, y, z, t)$ is the heat source field, x, y, z are the coordinates, and t is the time.

The IR camera allows one to register the temperature distribution only over the specimen surface that is the reason why Eq. 2 has to be averaged over the z-coordinate (thickness).



Difference $\theta'(x, y, t)$ between the averaged specimen temperature $T(x, y, z, t)$ and the initial specimen temperature in the thermal balance with the environment T_0 is defined as:

$$\theta'(x, y, t) = \frac{1}{b} \int_{-b/2}^{b/2} (T(x, y, z, t) - T_0) dz = \theta(x, y, t) - T_0 \quad (3)$$

where b is the specimen thickness.

The following boundary conditions are considered:

$$\begin{aligned} \left. \frac{\partial T(x, y, z, t)}{\partial x} \right|_{z=\frac{b}{2}} &= -\left. \frac{\partial T(x, y, z, t)}{\partial z} \right|_{z=-\frac{b}{2}} \\ -k \left. \frac{\partial T(x, y, z, t)}{\partial z} \right|_{z=\frac{b}{2}} &= \beta \int_{-b/2}^{b/2} (T(x, y, z, t) - T_0) dz \end{aligned} \quad (4)$$

where β is the heat exchange coefficient in perpendicular direction to the specimen surface. One boundary condition describes the symmetry of the heat source, whereas the second boundary condition is responsible for the heat exchange of the specimen with the environment.

Therefore, integrating Eq. (2), considering expressions (3) and boundary conditions (4), we obtain relation (5) to estimate the heat source field caused by irreversible deformation:

$$Q_{\text{int}}(x, y, t) = \rho c \left(\dot{\theta}(x, y, t) + \frac{\theta(x, y, t) - T_0}{\tau} \right) - k \Delta \theta(x, y, t) \quad (5)$$

where τ is the time constant, which is related to the heat losses [27, 28]. The parameter τ was measured before each test by the additional experimental procedure of specimen cooling after pulse point heating. The identification process consisted in estimating the time derivative and the Laplacian of the temperature function if there was no internal and external heat source on the specimen during its cooling. For steel AISI 304, the value of parameter τ amounted to 10 sec. The numerical finite-difference scheme of Eqn. (5) applied to the IR thermography data allows one to investigate the heat source evolution on the specimen surface. To calculate the heat sources from the noisy temperature fields, the procedure of the movement compensation and filtering of infrared data was performed. These algorithms are described in detail in [9].

Estimation of the dissipated energy based on the lock-in thermography

Energy dissipation can be estimated by applying the lock-in thermography technique. Lock-in thermography is based on a correlation in frequency, amplitude and phase of the detected signal with a reference signal coming from the loading system. Temperature variations on the specimen surface are monitored with the IR camera during mechanical tests. The evaluation of the dissipated energy is based on post-processing of the recorded thermal data using the Discrete Fourier Transformation (Eq. 6) and performed for each pixel of the recorded frames.

$$T(t) = T_m + T_E \cdot \sin(2\pi f_L \cdot t + \varphi_E) + T_D \cdot \sin(2 \cdot 2\pi f_L \cdot t + \varphi_D) + \Phi(t) \quad (6)$$

where T_m is the mean temperature, f_L is the mechanical loading frequency, φ_E and φ_D are the phase shifts, T_E is the thermo-elastic amplitude (E-mode), T_D is the plasticity effect amplitude (D-mode), and $\Phi(t)$ is the noise of the temperature signal.

It was shown that in case of plastic deformation the second mode coupled with the double loading frequency (D-mode) correlated with the dissipative energy [14].

Eq. (6) is integrated in the algorithm of Altair LI software. For each analysed sequence of IR frames, the evaluation provides an amplitude and a phase image for different modes.

RESULTS AND DISCUSSION

In order to compare the heat flux sensor results and the results of thermography measurements, we have studied the temperature evolution in a small rectangular area which covered all temperature fluctuations near the crack tip. The size of the area coincides with heat flux sensor dimensions.

A comparison of the results obtained by contact sensor and the infrared thermography data (heat conduction Eqn. (5)) during crack propagation tests is illustrated in Fig. 2. The heat flux sensor allows measurement of the integral heat flux only. The infrared thermography technique was used to obtain the image of temperature distribution and the field of heat source distribution in the crack tip region. To compare the IR results with the data of the contact sensor, we integrated the heat source field over the space equal to the size of contact sensor. Fig. 2a presents the characteristic curve describing the heat flux variation during the fatigue tests: solid line - heat flux measured by the contact heat flux sensor, squares - heat flux measured by the infrared thermography technique.

Three zones were identified on the heat flux curve during the crack propagation experiment. The short initial increasing zone corresponds to the crack initiation stage. The second zone with a constant heat flux corresponds to the steady state crack growth stage. The last zone is characterized by a sharp increase in heat dissipation and is ended with specimen failure. It can be seen that the power heat source detected by the contact sensor and determined on the basis of IR thermography data (Eqn. (5)) are in good quantitative agreement throughout the test.

Figs. 2b,c present the relation between the heat flux power (Q) and crack growth rate (da/dN) for the stainless steel AISI 304 specimen. The power law relation for predicting the fatigue crack growth is determined as follows:

$$\frac{da}{dN} = aQ_{\text{int}}^b. \quad (6)$$

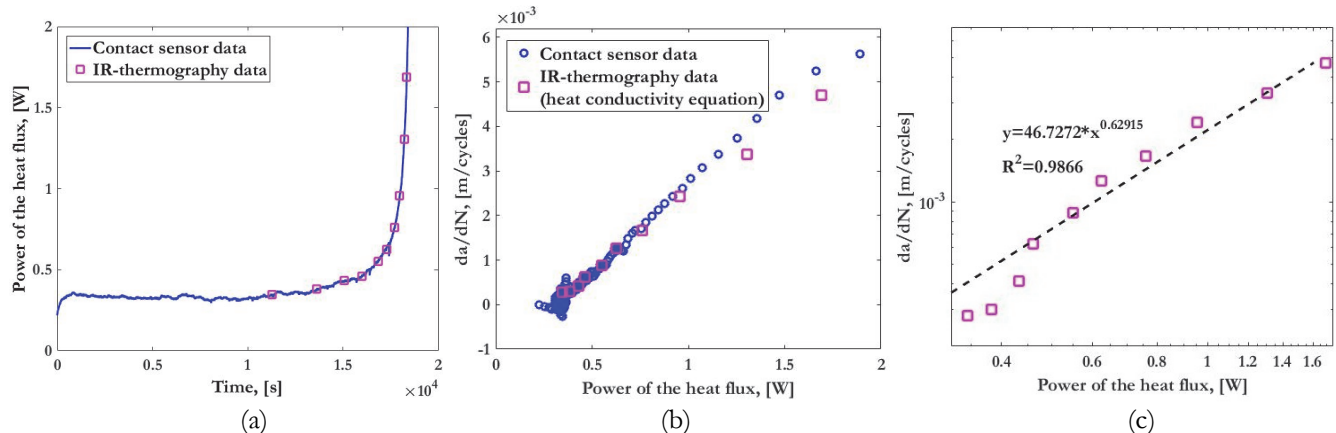


Figure 2: (a) IR-thermography data and heat flux sensor measurements; (b) heat flux power during crack propagation experiments; (c) relation between heat flux power and crack growth rate for the stainless steel AISI 304 specimen.

The obtained results led us to conclude that the techniques applied to estimate heat dissipation on the basis of contact and non-contact measurements can be used in engineering practice for fatigue crack growth predictions. Let us now consider the possibility of using lock-in thermography to predict fatigue crack growth. With the Altair LI software it is possible to calculate the resulting amplitude of temperature variations (amplitude image) and the distribution of phase shifts between the thermographic signal and the mechanical loading (phase image) for the E-mode and D-mode, respectively (Eq. 6). As shown by Bremond [13], the D-mode provides information about the dissipated energy. The values of the amplitude related to the double loading frequency were determined. Fig. 3a shows the results of the normalized lock-in thermographic and the heat flux sensor measurements of the crack propagation experiment with a constant force exerted on the stainless steel AISI 304 specimen. For normalization of lock-in thermography data, a scaling factor was used. We assume a linear relationship between each point of thermography data and the results of the contact heat flux sensor. The scaling factor is computed for one point as the ratio of the power of heat source obtained by contact sensor to the value of D-amplitude. Then the values of D-amplitude at other time moments are multiplied by a scaling factor. For steel AISI 304, the value of scaling factor amounts to 0.32. It can be seen that the dissipated energy measured by lock-in



thermography and the heat flux sensor are in good qualitative agreement over the high heat dissipation period. The averaged D-Amplitude values are rising with loading cycles what caused by processes in front of the crack tip.

The D-amplitude behaviour and, in particular, its increase are similar to that of the crack growth rate. Therefore, the value of the D-mode amplitude can be used to describe crack propagation.

Figs.3b,c present the relation between D-mode variation and crack growth rate for the stainless steel AISI 304 specimen. The power law relation is determined as follows:

$$\frac{da}{dN} = aS_d^b \quad (7)$$

where S_d is the maximum amplitude of the thermal signal that changes at the double of loading frequency.

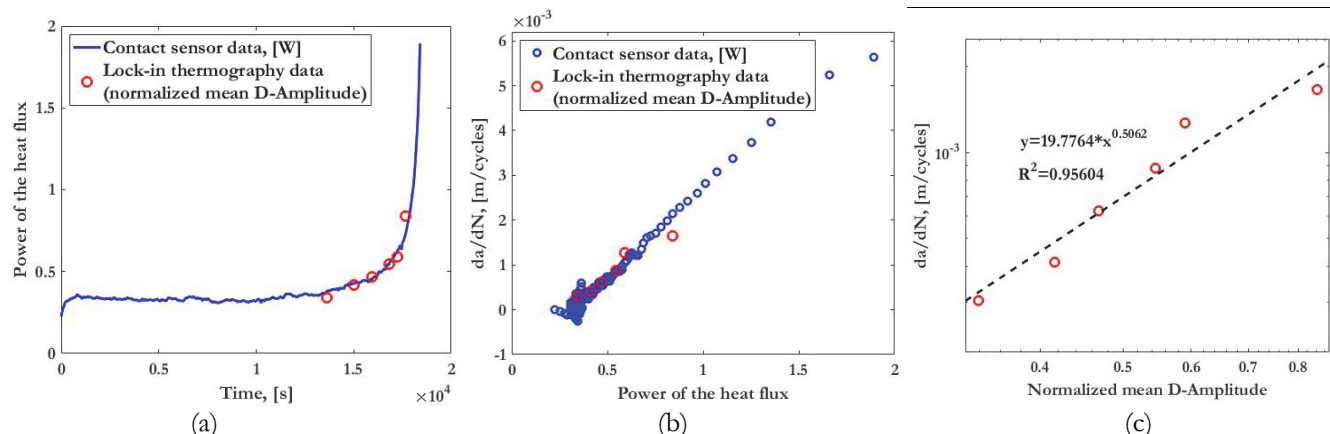


Figure 3: (a) lock-in thermography data and heat flux sensor measurements; (b) heat flux during crack propagation experiments; (c) relation between second order temperature variation and crack growth rate for the stainless steel AISI 304 specimen.

Analysis of the results has revealed that lock-in thermography can be used for evaluating the crack growth rate. It is interesting that the fatigue crack growth can be described by the D-amplitude signal in very similar to the Paris Law.

CONCLUSION

R-thermography data, lock-in thermography data and heat flux sensor measurements were used to investigate energy dissipation under fatigue crack propagation in stainless steel AISI 304. Comparison of the obtained results demonstrates that they are in good qualitative agreement. At the scaling factor of 0.32 the heat flux sensor results coincide quantitatively with the lock-in thermography data. The thermographic and heat flux sensor measurements showed an increase in the energy dissipated ahead of the crack tip with increasing crack growth rate. The measured energy dissipation values can be used to determine a linear correlation between these two parameters.

ACKNOWLEDGMENTS

This work was supported by the Russian Foundation for Basic Research (grant №18-31-00293) and the Presidium of the Russian Academy of Sciences (program no. 16 “Development of Physicochemical Mechanics of Surface Phenomena as the Fundamental Basis for the Development of Modern Structures and Technologies”).

REFERENCES

- [1] Iziumova, A., Plekhov, O. (2014). Calculation of the energy J-integral in plastic zone ahead of a crack tip by infrared scanning, *Fatigue Fract. Eng. Mater. Struct.*, 37, pp. 1330-1337. DOI: 10.1111/ffe.12202.



- [2] Vshivkov, A., Iziumova, A., Plekhov, O., Bär, J. (2016). Experimental study of heat dissipation at the crack tip during fatigue crack propagation, *Frat. Ed Integrita Strutt.*, 35, pp. 131-137. DOI: 10.3221/IGF-ESIS.35.07.
- [3] Pradere, C., Joanicot, M., Batsale, J.-C., Toutain, J., Gourdon, C. (2007). Processing of temperature field in chemical microreactors with infrared thermography, *Quant. Infrared Thermogr. J.*, 3, pp. 117-135. DOI: 10.3166/qirt.3.117-135.
- [4] Wang, C., Blanche, A., Wagner, D., Chrysochoos, A., Bathias, C. (2014). Dissipative and microstructural effects associated with fatigue crack initiation on an Armco iron, *Int. J. Fatigue*, 58, pp. 152-157. DOI: 10.1016/j.ijfatigue.2013.02.009.
- [5] Izyumova, A.Y., Plekhov, O.A., Vshivkov, A.N., Prokhorov, A.A., Uvarov, S. V. (2014). Studying the rate of heat dissipation at the vertex of a fatigue crack, *Tech. Phys. Lett.*, 40, pp. 810-812. DOI: 10.1134/s1063785014090211.
- [6] Iino, Y. (1979). Fatigue crack propagation work coefficient-a material constant giving degree of resistance to fatigue crack growth, *Eng. Fract. Mech.*, 12, pp. 279-299. DOI: 10.1016/0013-7944(79)90120-6.
- [7] Chow, C.L., Lu, T.J. (1991). Cyclic J-integral in relation to fatigue crack initiation and propagation, *Eng. Fract. Mech.*, 39, pp. 1-20. DOI: 10.1016/0013-7944(91)90018-V.
- [8] Dowling, N., Begley, J. (1976). Fatigue Crack Growth During Gross Plasticity and the J-Integral. *Mechanics of Crack Growth*, ASTM STP, 590, pp. 80-103.
- [9] Fedorova, A.Y., Bannikov, M. V., Terekhina, A.I., Plekhov, O.A. (2014). Heat dissipation energy under fatigue based on infrared data processing, *Quant. Infrared Thermogr. J.*, 11(1), pp. 2-9. DOI: 10.1080/17686733.2013.852416.
- [10] Plekhov, O.A., Saintier, N., Palin-Luc, T., Uvarov, S. V., Naimark, O.B. (2007). Theoretical analysis, infrared and structural investigations of energy dissipation in metals under cyclic loading, *Mater. Sci. Eng. A*, 462(1-2), pp. 367-369. DOI: 10.1016/j.msea.2006.02.462.
- [11] Iziumova, A., Vshivkov, A., Prokhorov, A., Plekhov, O., Venkatraman, B. (2016). Study of heat source evolution during elastic-plastic deformation of titanium alloy Ti-0.8Al-0.8Mn based on contact and non-contact measurements, *PNRPU Mech. Bull.*, 1, pp. 68-81. DOI: 10.15593/perm.mech/2016.1.05.
- [12] Plekhov, O., Vshivkov, A., Iziumova, A., Zakharov, A., Shlyannikov, V. (2019). The experimental study of energy dissipation during fatigue crack propagation under biaxial loading, *Frat. Ed Integrita Strutt.*, 48, pp. 50-57. DOI: 10.3221/IGF-ESIS.48.07.
- [13] Brémond, P. (2007). New developments in Thermo Elastic Stress Analysis by Infrared Thermography. IV Pan-American Conference for Non Destructive Testing, Buenos Aires, Argentina, 22-26 October.
- [14] Sakagami, T., Kubo, S., Tamura, E., Nishimura, T. (2005). Identification of plastic-zone based on double frequency lock-in thermographic temperature measurement. International conference of fracture ICF 11, Turin, Italy, 20-25 March.
- [15] Bär, J. (2016). Determination of dissipated Energy in Fatigue Crack Propagation Experiments with Lock-In Thermography and Heat Flow Measurements, *Procedia Struct. Integr.*, 2, pp. 2105-2112. DOI: 10.1016/j.prostr.2016.06.264.
- [16] De Finis, R., Palumbo, D., Ancona, F., Galietti, U. (2017). Fatigue behaviour of stainless steels: A multi-parametric approach. *Conference Proceedings of the Society for Experimental Mechanics Series*, 9, pp. 1-8.
- [17] De Finis, R., Palumbo, D., Galietti, U. (2018). Energetic approach to study the plastic behaviour in CT specimens. 14th Quantitative InfraRed Thermography Conference, Berlin, Germany, 25-29 June. DOI: 10.21611/qirt.2018.133.
- [18] Bär, J., Seifert, S. (2014). Investigation of Energy Dissipation and Plastic Zone Size During Fatigue Crack Propagation in a High-Alloyed Steel, *Procedia Mater. Sci.*, 3, pp. 408-413. DOI: 10.1016/j.mspro.2014.06.068.
- [19] Bär, J., Seifert, S. (2014). Thermographic Investigation of Fatigue Crack Propagation in a High-Alloyed Steel, *Adv. Mater. Res.*, 891-892, pp. 936-941. DOI: 10.4028/www.scientific.net/amr.891-892.936.
- [20] Bär, J. (2016). Determination of dissipated Energy in Fatigue Crack Propagation Experiments with Lock-In Thermography and Heat Flow Measurements, *Procedia Struct. Integr.*, 2, pp. 2105-2112. DOI: 10.1016/j.prostr.2016.06.264.
- [21] Bär, J., Urbanek, R. (2019). Determination of dissipated Energy in Fatigue Crack Propagation Experiments with Lock-In Thermography, *Frat. Ed Integrita Strutt.*, 48, pp. 563-570. DOI: 10.3221/IGF-ESIS.48.54.
- [22] Palumbo, D., De Finis, R., Galietti, U. (2019). Evaluation of the heat dissipated around the crack tip of AISI 422 and CF3M steels by means of thermography, *Procedia Struct. Integr.*, 18, pp. 875-885. DOI: 10.1016/j.prostr.2019.08.238.
- [23] Rigon, D., Ricotta, M., Meneghetti, G. (2019). Analysis of dissipated energy and temperature fields at severe notches of AISI 304L stainless steel specimens, *Frat. Ed Integrita Strutt.*, 47, pp. 334-347. DOI: 10.3221/IGF-ESIS.47.25.
- [24] Plekhov, O., Vshivkov, A., Iziumova, A., Venkatraman, B. (2019). A model of energy dissipation at fatigue crack tip in metals, *Frat. Ed Integrita Strutt.*, 48, pp. 451-458. DOI: 10.3221/IGF-ESIS.48.43.



- [25] Plekhov, O., Vshivkov, A., Iziumova, A., Zakharov, A., Shlyannikov, V. (2019). The experimental study of energy dissipation during fatigue crack propagation under biaxial loading, Frat. Ed Integrita Strutt., 48, pp. 50-57. DOI: 10.3221/IGF-ESIS.48.07.
- [26] Nayeb-Hashemi, H., Swet, D., Vaziri, A. (2004). New electrical potential method for measuring crack growth in nonconductive materials, Meas. J. Int. Meas. Confed., 36(2), pp. 21-129. DOI: 10.1016/j.measurement.2004.05.002.
- [27] Boulanger, T., Chrysochoos, A., Mabru, C., Galtier, A. (2004). Calorimetric analysis of dissipative and thermoelastic effects associated with the fatigue behavior of steels, Int. J. Fatigue, 26, pp. 221-229. DOI: 10.1016/S0142-1123(03)00171-3.
- [28] Chrysochoos, A., Louche, H. (2000). Infrared image processing to analyze the calorific effects accompanying strain localization, Int. J. Eng. Sci., 38, pp. 1759-1788. DOI: 10.1016/S0020-7225(00)00002-1.